Published in final edited form as:
Langmuir. 2011 February 15; 27(4): 1419–1429. doi:10.1021/la103975s.

Ordering Transitions in Nematic Liquid Crystals Induced by Vesicles Captured through Ligand-Receptor Interactions

Lie Na Tan[†], **Paul J. Bertics**[‡], and **Nicholas L. Abbott**[†,*]

[†]Department of Chemical and Biological Engineering, University of Wisconsin-Madison, 1415 Engineering Drive, Madison, Wisconsin 53706

[‡]Department of Biomolecular Chemistry, University of Wisconsin-Madison, 1300 University Avenue, Madison, Wisconsin 53706

Abstract

We report that phospholipid vesicles incorporating ligands, when captured from solution onto surfaces presenting receptors for these ligands, can trigger surface-induced orientational ordering transitions in nematic phases of 4′-pentyl-4-cyanobiphenyl (5CB). Specifically, whereas avidin-functionalized surfaces incubated against vesicles comprised of 1,2-dioleoyl-sn-glycero-3-phosphocholine (DOPC) were observed to cause the liquid crystal (LC) to adopt a parallel orientation at the surfaces, the same surfaces incubated against biotinylated vesicles (DOPC and 1,2-dioleoyl-sn-glycero-3-phosphoethanolamine-N-(biotinyl) (biotin-DOPE)) caused homeotropic (perpendicular) ordering of the LC. The use of a combination of atomic force microscopy (AFM), ellipsometry and quantitative fluorimetry, performed as a function of vesicle composition and vesicle concentration in solution, revealed the capture of intact vesicles containing 1% biotin-DOPE from buffer at the avidin-functionalized surfaces; subsequent exposure to water prior to contact with the LC, however, resulted in rupture of the majority of vesicles into interfacial multilayer assemblies with a maximum phospholipid loading set by random close-packing of the intact vesicles captured initially on the surface (5.1 ± 0.2 phospholipid molecules/nm^2). At high concentrations of biotinylated lipid (> 10% biotin-DOPE) in the vesicles, the limiting lipid loading was measured to be 4.0 ± 0.3 phospholipid molecules/nm^2, consistent with the maximum phospholipid loading set by spontaneous formation of a bilayer during incubation with the biotinylated vesicles. Independent of the initial morphology of the phospholipid assembly captured on the surface (intact vesicle, planar multilayer), we measured homeotropic ordering of the LC on the surfaces. We interpret this result to infer reorganization of the phospholipid bilayers either prior to or upon contact with the LCs such that interactions of the acyl chains of the phospholipid and the LC dominate the ordering of the LC, a conclusion that is further supported by quantitative measurements of the orientation of the LC as a function of surface density of phospholipid (>1.8 molecules/nm^2 is required to cause homeotropic ordering of the LC). These results and others presented herein provide fundamental insights into the interactions of phospholipid-decorated interfaces with LCs, and thereby provide guidance for the design of surfaces on which phospholipid assemblies captured through ligand-receptor recognition can be reported via ordering transitions in LCs.

[*] To whom all correspondence should be addressed. Tel: 608-265-5278. Fax: 608-262-5434. abbott@engr.wisc.edu.

Supporting Information Available. Experimental details related to the AFM imaging, fluorimetric measurements, optical micrographs of LCs and calculations are included. This information is available free of charge via the Internet at http://pubs.acs.org

Introduction

Microvesicles (or native vesicles) are membrane fragments comprised of various lipids and other plasma membrane-associated molecules that are shed from cell surfaces. Microvesicles are believed to play a role in mediating intercellular communication by facilitating transfer of bioactive molecules between cells.[1,2] It has also recently been reported that an elevated level of microvesicle shedding can be associated with cellular dysfunction and thus molecular analysis of microvesicles has the potential to reveal biological information pertaining to cells that shed microvesicles.[3,4] For example, it was shown that microvesicles shed by transformed glioma cells incorporate a mutant form of the epidermal growth factor receptor (EGFRvIII), which is often expressed in malignant brain tumors.[3] Accompanying the growing recognition of the biological significance of microvesicles is the need for general and facile methods that will permit the reporting of the presence of microvesicles shed from cells. Towards this goal, the present study investigates the capture of model phospholipid vesicles on surfaces via specific binding events, and the influence of the captured vesicles (or, more precisely, as revealed in this paper, phospholipid assemblies that are formed from the captured vesicles) on ordering transitions induced in nematic liquid crystals (LCs).

Many recent studies have demonstrated that surface-driven ordering transitions in LCs can be used as a means to amplify interfacial molecular events.[5-14] These investigations have revealed that the orientational ordering of LCs is influenced by the chemical functionality of interfaces via interactions such as hydrogen bonds[5], the presence of electrical double layers[6] and metal-ligand interactions[7]. Due to the elastic nature of LCs, surface-induced ordering of the molecules in LCs can propagate across micrometer-thick films. The optical birefringence of the LC films allows changes in the ordering of the LCs to be transduced into optical signals that are readily observed under a polarized light microscope. These principles have been used to report phenomena involving a range of different types of biomolecules at interfaces, including binding events involving proteins, peptides and nucleic acids.[8-14] Here we extend these principles to report ordering transitions in LCs that are triggered by assemblies of phospholipids that are captured at surfaces through specific binding events (see below for comments regarding past studies of lipid-induced ordering transitions in LCs).

The investigation described in this paper builds from prior studies that have reported on the ordering of LCs at surfaces decorated with phospholipids.[11,15-18] In particular, early work by Hiltrop and Stegemeyer demonstrated that the ordering of LCs at surfaces can be influenced by the presence of monolayers of lecithin transferred onto the surfaces by the Langmuir-Blodgett (LB) technique.[15,16] More recently, the influence of surfactants and phospholipids self-assembled at aqueous-LC interfaces on the ordering of LCs has been reported.[11,17-19] These past studies, when combined, suggest a physical picture in which monolayer films of phospholipids organize to present their hydrophobic tails towards the LC phase, thus leading to interdigitation of mesogens and lipid acyl chains with the subsequent homeotropic (perpendicular) ordering of the LCs. While these studies clearly demonstrate the influence of phospholipid-decorated surfaces on the ordering of LCs, the current work departs from these past investigations in two key aspects. First, the surfaces in the current study are decorated with phospholipids as a consequence of a receptor-mediated binding event (the previous reports identified above did not involve the capture of lipids at surfaces through specific recognition events). Second, the surfaces used in our study are decorated initially with vesicles (lipid bilayers) and not monolayers of phospholipids as reported in past studies.

We note that several past studies have provided detailed accounts of the behaviors of vesicles on surfaces.[20-22] Some of these investigations have been motivated by the potential utility of vesicles as amplifiers in analytical methods.[23] The approach we report here builds, in part, from prior reports of the capture of biotinylated vesicles on avidin-functionalized surfaces.[24-27] When the mole fraction of biotinylated lipid within the vesicles is low, biotinylated vesicles have been found to bind to avidin-functionalized surfaces and give rise to intact, surface-immobilized vesicles.[25-27] In this paper, we go beyond these past studies by characterizing changes in morphology of surface-bound vesicles that result from subsequent treatments (e.g., rinsing with water) of the bound vesicles. In addition, we determine if the changes in morphology of the vesicles observed in our experiments result in changes in the total loading of phospholipid on the surfaces (which would impact the subsequent ordering of LCs). We also quantify the influence of the interfacial concentration of phospholipid on ordering transitions of LCs in contact with the surfaces, and compare these measurements to past studies of the ordering of LCs on Langmuir-Blodgett films[15,16] and at LC-aqueous interfaces.[11,18]

Experimental Section

Materials

3-Aminopropyltriethoxysilane (APTES), Tris-buffered saline (TBS) (0.05 M TRIS; 0.138 M NaCl; 0.0027 M KCl; pH 8.0), phosphate-buffered saline (PBS) (0.01 M phosphate; 0.138 M NaCl; 0.0027 M KCl; pH 7.4), chloroform and octyltrichlorosilane (OTS) were obtained from Sigma-Aldrich (St Louis, MO). Heptane was obtained from Fisher Scientific (Pittsburgh, PA). Absolute ethanol (anhydrous, 200 proof) was purchased from Pharmco-AAPER (Shelbyville, KY). Biotinylated bovine serum albumin (biotin-BSA) and avidin were obtained from Pierce (Rockford, IL). 1,2-dioleoyl-sn-glycero-3-phosphocholine (DOPC) and 1,2-dioleoyl-sn-glycero-3-phosphoethanolamine-N-(biotinyl) (biotin-DOPE) were purchased from Avanti Polar Lipids, Inc (Alabaster, AL). N-(4,4-difluoro-5,7-dimethyl-4-bora-3a,4a-diaza-s-indacene-3-propionyl)-1,2-dihexadecanoyl-sn-glycero-3-phosphoethanolamine triethylammonium salt (BODIPY-DHPE) was obtained from Molecular Probes (Eugene, OR). The nematic LC 4′-pentyl-4-cyanobiphenyl (5CB) was obtained from EMD Chemicals (Spring Valley, NY). Deionization of a distilled water source was performed with a Milli-Q system (Millipore, Bedford, MA) to give water with a resistivity of 18.2 MΩ-cm. Fisher's Finest Premium Grade glass slides were purchased from Fisher Scientific (Hamton, NH). Polished Si wafers were purchased from Silicon Sense, Inc (Nashua, NH).

Preparation of Avidin-Functionalized Surfaces

Piranha-cleaned glass microscope slides (cleaned according to published procedures[28]) were surface-modified by immersion into an aqueous solution of 10 vol % APTES for 50 min at 80 °C. The slides were rinsed thoroughly with deionized water and dried with a stream of nitrogen gas. Next, a solution of 2.5 mg/ml biotinylated bovine serum albumin (biotin-BSA) in PBS buffer was incubated on the surface of the slides for 1 h. After thorough rinsing with PBS buffer and deionized water, the slides were incubated with an avidin solution (1 mg/ml in PBS) for 45 min.

Preparation of Octyltrichlorosilane(OTS)-Treated Glass Slides

Piranha-cleaned glass slides were immersed in a 10 mM solution of OTS in anhydrous n-heptane. After 30 min, each slide was rinsed with methylene chloride, a copious amount of water, and dried under a stream of nitrogen. The quality of the OTS layer was assessed by checking the alignment of 5CB between two OTS-treated glass slides.

Preparation of Phospholipid Vesicles

Briefly, biotin-DOPE and DOPC (dissolved in chloroform) were dispensed into glass vials in volumes that gave the desired concentration and biotin composition upon resuspension. The solution was dried using a stream of nitrogen to remove the chloroform. This was followed by addition of a known amount of BODIPY-DHPE (dissolved in ethanol) such that the final composition of BODIPY-DHPE in the phospholipid mixture was 1 mol %. After drying with a stream of nitrogen, the vial was placed under vacuum for at least 3 h. The dried lipid was resuspended in an aqueous solution of TBS (0.05 M Tris; 0.138 M NaCl; 0.0027 M KCl) and the resulting suspension was subjected to five freeze-thaw/vortex cycles. Unilamellar vesicles were formed by extruding the suspension several times through a polycarbonate membrane (100 nm filter) (Millipore, Bedford, MA). The vesicles were used within 24 h of their preparation.

Dynamic Light Scattering Measurements

A 100 mW, 532 nm laser (Coherent Compass 315M-100) illuminated a temperature-controlled glass cell at 25 °C filled with a refractive-index matching fluid (decahydronaphthalene, Fisher Scientific, Pittsburgh, PA). The angle of the detector was set at 90°. The autocorrelation function (ACF) was obtained using BI-9000AT digital autocorrelator (Brookhaven Instruments Corporation, Holtsville, NY) and analyzed using the CONTIN[29,30] software package to yield a distribution of aggregate sizes.

Ellipsometry

A Rudolph Auto EL ellipsometer (wavelength of 632 nm, 70° angle of incidence) was used to determine the optical thicknesses of layers of APTES, biotin-BSA, avidin on Si surfaces as well as the avidin-functionalized surfaces on which solution of vesicles had been incubated. Ellipsometric constants were determined at five locations on each sample. A simple slab model was used to interpret these constants. The slab was assumed to have an index of refraction of 1.46.[31]

Epifluorescence Imaging of Surfaces

Surfaces, after incubation against fluorescently-labeled vesicles, were imaged by epifluorescence microscopy using an Olympus IX71 inverted microscope equipped with a 100 W mercury lamp. A fluorescence filter cube with excitation at 480 nm and emission at 535 nm (Chroma, Rockingham, VT) was used to visualize BODIPY FL fluorescence. Images were collected with a Hamamatsu 1394 ORCA-ER CCD camera (Bridgewater, NJ) connected to a computer and controlled through SimplePCI imaging software (Compix Inc., Cranberry Twp., NJ). Fluorescence imaging was performed using an objective power of 4× and an exposure time of 2.0 sec. All fluorescence intensity measurements were corrected for background fluorescence, measured using avidin-functionalized surfaces. Intensity values were determined using ImageJ (public-domain image processing software by the U.S. National Institutes of Health).

Quantification of the Interfacial Concentration of Phospholipid via Fluorimetric Measurements

Fluorimetric measurements were performed using a FluoroMax-3 fluorimeter (Instruments S. A./Jobin Yvon/Spex Horiba Group, Edison, NJ) with an excitation wavelength of 480 nm (0.5 nm excitation slit) and an emission wavelength range of 490–550 nm (5 nm emission slit) for the detection of BODIPY fluorescence. The fluorimeter was connected to a computer and controlled using DATAMAX software (Instruments S. A./Jobin Yvon/Spex Horiba Group).

To determine the interfacial concentration of phospholipid on a surface, the following procedure was used.[32] First, solutions of known concentrations of vesicles containing 1 mol % BODIPY-DHPE were mixed with 0.5% (v/v) Triton X-100. A calibration curve of fluorimetric intensity versus known phospholipid concentration was established. Next, surfaces that had been incubated against vesicle solutions composed of 1 mol % BODIPY-DHPE were rinsed thoroughly using 1 mL of 0.5% (v/v) Triton X-100 in TBS buffer to extract the phospholipids from the surface into the Triton X-100 solution. Epifluorescence imaging of surfaces was used to confirm that the phospholipids were stripped from the surface. The extract was collected in a cuvette and fluorimetric measurements were used to determine the concentration of phospholipid in each sample. Combined with the knowledge of the area of the surfaces, the above measurements were used to calculate the interfacial concentration of phospholipid. Control experiments using surfaces that had not been contacted with the vesicle solutions were performed to determine the background fluorescence.

Atomic Force Microscopy

AFM experiments were carried out with a Nanoscope III Multimode scanning probe microscope equipped with a "J" (120 μm) scanner (Veeco/Digital Instruments, Santa Barbara, CA). The images were acquired in tapping mode in solution using a commercially available liquid cell with oxide-sharpened silicon nitride V-shaped cantilevers at room temperature. The cantilever had a nominal spring constant of 0.32 N/m. Imaging was performed at a scan rate of 2 Hz and at a resolution of 256 pixels/line. Images were flattened as required.

Characterization of the Surface-Induced Ordering of LCs

Optical cells were fabricated from two glass slides, one of which was OTS-treated. The other surface was avidin-functionalized and incubated against a solution of vesicles. The surfaces of the glass slides were aligned facing each other, and were clipped together using a thin film of Saran Wrap (thickness ≈ 18 μm) at the edge to space the two surfaces apart. A drop of 5CB at room temperature was introduced into the cavity between the two surfaces of the optical cell and drawn inwards by capillary forces. The cell was subsequently incubated at 36 °C (corresponding to the isotropic phase of 5CB) and then cooled gradually to room temperature before observing the optical texture.

Polarized Light Microscopy

The orientation of 5CB in the optical cells described above was examined by using plane-polarized light in transmission mode on an Olympus BX-60 microscope with crossed polarizers. Each optical cell was placed on a rotating stage located between the polarizers. In-plane birefringence was determined by rotating the stage by 45° and observing the modulation in the intensity of transmitted light. Homeotropic (perpendicular) alignments of LC were determined first by the absence of transmitted light during a 360° rotation of the sample. Second, insertion of a condenser lens below the stage and a Bertrand lens above the stage allowed conoscopic examination of the LC. An interference pattern consisting of two crossed isogyres observed in the back focal plane indicated homeotropic alignment.[33] Images were captured with a microscope-mounted digital camera (Olympus C-2040 Zoom) set to an f-stop of 2.8 and a shutter speed of 1/320 sec.

Results

Characterization of biotinylated vesicles captured on avidin-functionalized surfaces

Prior to characterizing the orientational ordering of LCs on surfaces onto which vesicles were captured, we verified that the surfaces used in our study were decorated with avidin and that the incubation of biotinylated vesicles on these surfaces led to the capture of vesicles via biotin-avidin recognition. In the context of the second goal, we devoted particular attention to characterization of any changes in morphology of the surface-bound vesicles induced by exposure of the vesicles to water and air as well as quantification of any changes in the loading of phospholipid on the surfaces that accompanied changes in morphology.

The avidin-functionalized surfaces were prepared on silicon wafers with native oxide in order to measure the ellipsometric thicknesses. The native oxide on the surface of the silicon wafer was silanized by immersion into an aqueous solution of 10 vol % APTES, resulting in formation of a layer of APTES that was determined to be 0.8 ± 0.4 nm in thickness (Figure 1a). Subsequent incubation in biotinylated BSA (9 mole of biotin/mole BSA) resulted in an increment in ellipsometric thickness of 2.5 ± 0.9 nm, consistent with an adsorbed layer of biotinylated BSA.[34] Incubation of the surface functionalized with biotinylated BSA with avidin (1 mg/ml in PBS buffer) resulted in a further increment of 6.7 ± 1.2 nm in ellipsometric thickness. This increment, which corresponds approximately to the longest dimension of the avidin molecule (6.0 nm × 5.5 nm × 4.0 nm),[35] is consistent with the formation of a densely-packed layer of avidin. As a control, we repeated the experiment described above using BSA (not biotinylated BSA). This control experiment resulted in a negligible change in ellipsometric thickness upon incubation with avidin, thus confirming that the ellipsometric thickness of 6.7 ± 1.2 nm reported above results from biotin-mediated binding of avidin to the surface coated with biotinylated BSA. It is interesting to note that the change in thickness associated with binding of avidin (6.7 ± 1.2 nm) is substantially larger than the increment in thickness caused by adsorption of biotin-BSA (2.5 ± 0.9 nm). The relative magnitude of these ellipsometric thicknesses likely reflects the presence of multiple biotin groups (i.e., 9 potential binding groups for avidin) per BSA molecule on the surface. Finally, we note that AFM imaging of the avidin-functionalized surface revealed the topography of the surface to be relatively smooth (root-mean-square roughness of 0.97 nm measured over an area of 2 μm × 2 μm), consistent with our conclusion stated above that coverage of avidin is high (i.e., close to monolayer coverage; see Figure S1).

Next, we prepared unilamellar vesicles composed of either 98 mol % DOPC, 1 mol % biotin-DOPE and 1 mol % BODIPY-DHPE (biotinylated vesicles) or 99 mol % DOPC and 1 mol % BODIPY-DHPE (biotin-free vesicles) by extrusion to achieve a final phospholipid concentration of 0.2 mM. This procedure (see Materials and Methods for details) yielded an average vesicle diameter of 130 nm, as determined using dynamic light scattering (DLS). We note that we used DOPC to prepare the vesicles because it possesses a bilayer melting temperature that is below ambient (T_m = -20 °C)[36], thus facilitating reorganization of the phospholipid assemblies used in our studies. Solutions containing vesicles were incubated on the avidin-functionalized surfaces for 45 mins and then rinsed with TBS buffer. We also rinsed the surfaces with water and dried them under a stream of N_2 prior to placing them into contact with LCs. The surfaces were rinsed with water to remove buffering salts that we thought might deposit onto the surfaces during drying and thus impact the orientational ordering of the LCs.[6]

Quantification of the surface density of phospholipid captured on the avidin-functionalized surfaces (area 1 cm × 2.5 cm) was performed by extracting the adsorbed phospholipids with TBS buffer containing 0.5% (v/v) Triton X-100 (see Material and Methods for details).

After incubation of the avidin-functionalized surface with biotinylated vesicles, the density of phospholipid on the surface was determined to be 2.5 ± 0.3 molecules/nm^2 (see Figure S2). A slight decrease in surface density (to 2.2 ± 0.2 phospholipid molecules/nm^2) was measured when the surface was rinsed subsequently with distilled water. After drying, the final surface density was determined to be 2.1 ± 0.3 phospholipid molecules/nm^2, thus indicating that the combined effect of rinsing and drying was a loss of ~15% of the phospholipid initially captured onto the surface. Overall, these results indicate that phospholipid was captured on the avidin-functionalized surfaces upon incubation against solutions containing biotinylated vesicles (see the last paragraph of this section for control experiments that confirm the capture arises from biotin-avidin binding) and that transfer of the surface-bound phospholipid assemblies to water and air had only a small impact (~15%) on the phospholipid loading on the surface. We also comment that this areal density of phospholipid measured on the surfaces is comparable to monolayer coverage, a point that we will return to below.

To address the state of the phospholipid captured on the surfaces (and possible changes in morphology of lipid assemblies) and to provide insights into the possible reorganization of phospholipid prior to contact with LCs, we imaged the surfaces with AFM. All images were acquired in TBS buffer to avoid the effect of double layer repulsion which can result in height artifacts.[37] Following incubation of the avidin-functionalized surface against biotinylated vesicles (1% biotin-DOPE) and subsequent transfer into TBS buffer free of vesicles, the AFM images showed raised circular features which are identified as surface-bound vesicles (Figure 2a). The average height of individual vesicles was ~50 nm, consistent with the results obtained by Pignataro *et al.*[24] Because our DLS measurements revealed the diameter of the vesicles to be ~130 nm, this result suggests that the vesicles were adsorbed to the surfaces in a flattened configuration. The apparent diameter of the vesicles in the AFM images is ~200 nm, which is greater than that obtained from DLS and likely reflects the flattened configuration of the vesicles as well as tip convolution effects.[38] The key conclusion emerging from these measurements is that intact vesicles are present initially on the avidin-functionalized surfaces (Figure 3a).

After a surface analogous to that shown in Figure 2a was rinsed with distilled water and then returned to TBS for imaging, we observed the topographical features shown in Figure 2a to disappear. Instead, we measured the surface to possess patches that varied in height by ~4 nm (Figure 2b). This variation in height is consistent with the approximate thickness of a bilayer of DOPC.[39] We interpret these results to indicate that exposure of the surface-immobilized vesicles to water resulted in the rupture of the vesicles and formation of bilayer assemblies spread on the surface (Figure 3b).[40,41] We also note that not all vesicles-like features on the surface disappeared on exposure to water (Figure 2b, arrow).

We suspected the osmotic pressure difference generated across the bilayers of intact vesicles upon contact with water to be responsible for the rupture of the surface-bound vesicles. At equilibrium, the osmotic pressure difference, ΔP, across a membrane is balanced by the membrane tension τ, which is expressed by the Laplace equation as $\tau = \Delta P \cdot r/2$, where r is the vesicle radius. We calculated the membrane tension generated by the osmotic pressure across the bilayers in our experiments to be 8.5 mN/m, a value that is close to the lysis tension of DOPC vesicles (9.9 mN/m; see Supporting Information).[42] This interpretation (rupture of vesicles due to osmotic pressure difference) is consistent with a study by Schonherr *et al.*, who also concluded that osmotic pressure differences can rupture immobilized vesicles to form isolated bilayer disks.[21] Interestingly, our results, when combined with the above-described fluorimetric measurements of total phospholipid loading on the surfaces, reveal that the osmotic-induced rupture of vesicles does not lead to the loss of a substantial amount of phospholipid from the surface (~10% of the lipid is lost; see

above). We also suspect that the small population of vesicles that survive exposure to pure water (see Figure 2b) may be vesicles that are imperfect (i.e., contain defects that allow the passage of solutes) and thus prevent the formation of an osmotic pressure differential across the vesicle bilayer.

Prior to contact of the phospholipid-decorated surfaces with LC, we transferred the surfaces to air (and dried any residual water from the surface). Although we do not have direct experimental evidence, we postulate that the bilayer state of the phospholipid-decorated surfaces that we observe under TBS does not survive transfer to air.[43] It is probable that the bilayer reorganizes upon exposure to air to present the non-polar aliphatic chains of the phospholipids towards air and thereby minimize surface energy (Figure 3c). Such a reorganization of phospholipids has been reported by Solletti *et al.*[44] Those authors suggested that transfer of DPPE bilayers from water into air leads to a "flip-flop" reorganization of the upper monolayer to form bilayer domains superimposed on a homogeneous lower layer (as shown in Figure 3c).[44] Overall, Figure 3 presents a schematic illustration of our understanding of the states of the phospholipids on the surfaces used in our study prior to contact with the LC. Initially, vesicles are captured on the surface (Figure 3a); upon contact with water they rupture to form bilayers (Figure 3b); and upon drying, the bilayers reorganize to present the phospholipid tails to air (Figure 3c).

Although the measurements above clearly demonstrate that biotinylated vesicles were captured on the avidin-functionalized surfaces, we performed numerous control experiments using a combination of ellipsometry, epifluorescence imaging and fluorimetric measurements to confirm that the vesicles were indeed captured through specific binding of the biotin of the vesicles to avidin. All of these measurements were performed on surfaces that were rinsed with water and transferred to air, as described above. In brief, the ellipsometric thickness of the surface increased by 2.6 ± 0.2 nm following incubation against biotinylated vesicles. In contrast, within the error of measurement, no change in optical thickness was observed on the avidin-functionalized surface after incubation against biotin-free vesicles (Figure 1a). This control experiment supports our conclusion that biotinylated vesicles were captured on the surfaces via binding of biotin to avidin. Measurements of epifluorescence intensity also confirmed this conclusion (Figure 1b). Finally, incubation of biotinylated vesicles on BSA-functionalized surfaces (no avidin) led to negligible capture of phospholipid (see Figure S3), providing further evidence that the capture of the vesicles shown in Figure 2 was mediated by biotin-avidin recognition.

LC Ordering Transitions Induced by Phospholipid Vesicles Captured on Surfaces

We investigated the ordering of nematic 5CB on avidin-functionalized surfaces incubated against solutions of biotinylated vesicles (0.2 mM total phospholipid in solution), prepared as described in the preceding section. Contact of LC with each surface was achieved by assembling the surface into an optical cell. Details of the fabrication of the optical cells are described in the Methods section. In brief, an OTS-treated glass surface that induces homeotropic (perpendicular) ordering of 5CB was paired with the surface of interest (e.g., avidin-functionalized surface onto which vesicles had been captured). Figure 4a shows the result for a film of 5CB (crossed polars) in contact with an avidin-functionalized surface that had been incubated with biotin-free vesicles. The bright optical texture and presence of line defects in the LC suggest a planar or tilted ordering of 5CB at the surface. Upon rotation of the sample, the optical texture changed in brightness (see Figure S4).

To quantify the orientation of 5CB at the surface described above, we used a Berek compensator placed into the optical path between the sample and analyzer. From a measurement of the retardance and knowledge of the thickness of the film of 5CB, we calculated the effective birefringence of the film to be 0.096 ± 0.011. The effective

birefringence, Δn_{eff}, of a slab of LC can be related to the tilt angle, θ, of the optical axis of the LC (measured relative to the surface normal) by

$$\Delta n_{eff} = \frac{n_{\parallel} n_{\perp}}{\sqrt{n_{\perp}^2 \sin^2(\theta) + n_{\parallel}^2 \cos^2(\theta)}} - n_{\perp}$$

where $n_{\parallel}$ and $n_{\perp}$ are the indices of refraction parallel and perpendicular to the optical axis of 5CB, respectively. For the LC cells with avidin-functionalized surfaces incubated against biotin-free vesicles, however, the tilt angle of the LC is not uniform across the LC film (Figure 4b). Minimization of the elastic energy of the strained state of the LC within the film leads to the prediction that the tilt angle of the LC varies linearly from the OTS surface ($\theta_1 \sim 0°$) where z = 0 to the avidin-functionalized surface which had been incubated against solution of vesicles (θ_2; z = d).[45] Under these conditions, the effective birefringence of the film of 5CB can be calculated from the integral[45]

$$\Delta n_{eff} \approx \frac{1}{d} \int_0^d \left(\frac{n_{\parallel} n_{\perp}}{\sqrt{n_{\perp}^2 \sin^2(\frac{z}{d}\theta_2) + n_{\parallel}^2 \cos^2(\frac{z}{d}\theta_2)}} - n_{\perp} \right) dz$$

where *d* is the thickness of the LC film.

Using the above equation, we determined that the tilt angle θ_2 of the 5CB at the avidin-functionalized surface (incubated with biotin-free vesicles) was 93 ± 7°, thus corresponding to a planar orientation of the LC. This angle is indistinguishable from the angle measured on avidin-functionalized surfaces (not incubated in solutions of vesicles) and is consistent with our earlier conclusion (Figure 1) that little phospholipid is adsorbed to the avidin-functionalized surface upon incubation against biotin-free vesicles. Interestingly, we note that past studies have concluded that a variety of protein-functionalized surfaces give rise to planar/titled alignment of nematic 5CB. [8,9,12] Although this surface-induced orientation of 5CB appears to be common to a range of protein-coated surfaces, the intermolecular interactions between nematic 5CB and proteins that give rise to this orientation remain to be elucidated.

Figure 4c shows the optical appearance of nematic 5CB in contact with an avidin-functionalized surface that was incubated against biotinylated vesicles prior to contact with 5CB. The optical appearance of the 5CB is uniformly dark, and no modulation of the intensity of transmitted light was observed upon rotation of the sample between crossed polars. This result suggests homeotropic (perpendicular) ordering of the LC at the surface (Figure 4d), a conclusion that is supported by conoscopy (an interference pattern consisting of two crossed isogyres was observed).[33] As mentioned in the Introduction, several past studies have concluded that monolayers of amphiphilic molecules orient LCs largely through steric effects in which mesogens interdigitate into the aliphatic chains of the monolayers.[15-17,19] In contrast to these past studies, however, the phospholipids in our investigation were not delivered to the surfaces as monolayers but were captured as vesicles via specific binding interactions involving ligands (biotin) present on the surface of the vesicles. The observation of homeotropic ordering of the nematic 5CB observed in our study, however, does suggest that the interaction between the 5CB and phospholipid on the surfaces of our study involved the aliphatic tails. This conclusion is also consistent with the organization of phospholipids proposed in Figure 3c, in which the phospholipids have

rearranged to form assemblies on the surface that present the lipid acyl chains to the 5CB. Below, we explore in greater detail how the amount of phospholipid on these surfaces influences the ordering of the LC. Overall, the observation of homeotropic ordering reported above is promising given that the ordering of the LC on the avidin-functionalized surface after incubation against the biotinylated vesicles (Figure 4c) is clearly distinct from the ordering observed upon contact with biotin-free vesicles (Figure 4a).

Influence of Phospholipid Density on the LC Ordering Transition

To determine how the ordering of 5CB depends on the amount of phospholipid captured as vesicles on the surface, we incubated solutions of vesicles with varying total phospholipid concentrations (1 mol % biotinylated lipid) on the avidin-functionalized surfaces for 45 min. As shown in Figure 5a-c, the ellipsometric thickness, epifluorescence intensity and interfacial concentration of phospholipid molecules on the avidin-functionalized surfaces were measured to decrease with decreasing concentration of phospholipid in solution. For example, when the concentration of phospholipid in solution was lowered to 0.025 mM, the interfacial concentration of phospholipid was determined to be 0.19 ± 0.05 phospholipid molecules/nm^2.

To provide insight into the physical processes that control the amount of phospholipid captured on the surfaces, as shown in Figure 5a-c, we calculated the time required for vesicles to diffuse to the avidin-functionalized surface from solution. The diffusion time required to supply the phospholipids to the surface can be calculated as $t = h^2/D$, where D is the diffusion coefficient of the vesicles ($D = k_BT/6\pi\eta r \sim 3.8\cdot10^{-12}$ m^2/sec; see Supporting Information) and h is the characteristic adsorption depth. The adsorption depth is a measure of the distance over which the vesicles must diffuse to reach the coverage of phospholipid measured on the avidin-functionalized surface, and is defined as $h = \Gamma_{eq}/C_\infty$, where Γ_{eq} is the interfacial concentration and C_∞ is the bulk concentration of the phospholipid molecules.[46] To achieve monolayer coverage of phospholipid (~2 molecules/nm^2) with C_∞ = 0.025 mM, we determined h to be 1300 μm. The time t required for diffusion of vesicles across this adsorption depth was calculated to be ~1.3 h, suggesting that the amount of phospholipid captured on the surfaces (in Figure 5a-c) is likely limited by mass transfer. This conclusion is supported further by the observation that the interfacial density of phospholipid captured on the surface increased from 0.19 to 1.25 molecules/nm^2 when the incubation time of a solution containing 0.025 mM of phospholipid was increased from 45 min to 6 h (see Figure S5).

The orientational ordering of 5CB on the surfaces described above is shown in Figure 5d-g. For the surfaces incubated against solutions of biotinylated vesicles with a total lipid concentration of either 0.025 mM or 0.05 mM, the birefringence were measured to be 0.099 ± 0.012 and 0.097 ± 0.011, respectively. These values of birefringence correspond to tilt angles of the LC at the avidin-functionalized surfaces of 96 ± 9° and 95 ± 8°, respectively, thus indicating that the LCs were oriented close to parallel to both surfaces. The corresponding surface densities of phospholipid were 0.2 and 0.6 molecules/nm^2 (Figure 5c). Incubation of the solution containing a total phospholipid concentration of 0.1 mM led to a surface density of 0.9 ± 0.2 phospholipid molecules/nm^2, and the observation of spatially patterned orientations (planar and perpendicular) of the LC (Figure 5d). The patterned orientations of the LC on the surface likely arise from a non-uniform distribution of phospholipid on the surface, caused either by the rinsing of the surface and/or the flow of the LC across the phospholipid-laden surface. Finally, we note that uniform homeotropic coverage was observed for surfaces with an interfacial concentration of 2.1 ± 0.3 phospholipid molecules/nm^2.

From the above experiment, we derive two primary conclusions. First, the results suggest that a threshold amount of phospholipid equivalent to approximately a single monolayer is required to trigger the ordering transition in the LC (the density of DOPC in a close-packed monolayer is ~1.6 molecules/nm^2).[47] Several prior studies have suggested that LC-lipid interactions leading to the orientational ordering of LCs at LC-aqueous and solid interfaces are highly dependent on lipid area density.[16,18] For example, Meli and coworkers demonstrated that a dilauroylphosphatidylcholine (DLPC) monolayer with density >1.8 DLPC molecules/nm^2 would cause homeotropic alignment of nematic 5CB at an aqueous-5CB interface.[18] Our results with biotinylated vesicles captured at avidin-functionalized surfaces are in good agreement with this prior study (see the Discussion for a more exact value of the minimum density of phospholipid required to induce ordering transition in our system). The observation that the surface density of phospholipid required to drive the ordering transition of 5CB in our system is similar to values reported in past studies of monolayer-decorated interfaces thus provides further support for our conclusion that interactions involving the phospholipid acyl chains and 5CB are likely responsible for the ordering transitions observed in our studies. The second key observation emerging from our study is that the ordering transitions of 5CB that we observed as a function of surface density of phospholipid was discontinuous. We did not observe tilted orientations of the LC.

Inspection of Figure 5 reveals that the highest phospholipid loading in our experiments was 2.1 phospholipid molecules/nm^2. To understand if this represents an upper limit to the amount of phospholipid that can be captured on the avidin-functionalized surface, we performed experiments with higher concentrations of vesicles. Incubation of the avidin-functionalized surface with higher concentrations of vesicles revealed that the interfacial concentration reached a limiting value of 5.1 ± 0.2 phospholipid molecules/nm^2 (see Figure S6). By modeling vesicles as diffusion-limited hard spheres that randomly adsorb to a planar surface, Zhdanov *et al.* predicted the maximum surface coverage of vesicles to be 55-60% of the hexagonal close-packed value.[48] We calculated that a hexagonal close-packed arrangement of vesicles with a diameter of 130 nm would yield a surface density of 10.1 phospholipid molecules/nm^2, and thus that randomly adsorbed vesicles would yield an area density of 6.0 phospholipid molecules/nm^2 at saturation (see Supporting Information). This value is in reasonable agreement with the limiting value that we measured (5.1 phospholipid molecules/nm^2). The result suggests that the maximum surface loading of phospholipid in our experiments corresponds to randomly close-packed vesicles on the surface. We also note that our AFM measurements are suggestive of the possibility that the vesicles attached to the surface assume a flattened configuration – this consideration and others may account for the difference between the above calculated maximum lipid loading and the experimental observation. We also point out that homeotropic ordering of 5CB was observed on surfaces presenting these high surface loadings of phospholipid.

Effect of the composition (mol% biotinylated lipid) of vesicles on ordering transitions of LCs

Finally, we sought to quantify how the mole fraction of biotinylated lipid in the vesicles would influence the amount of phospholipid captured on the avidin-functionalized surfaces. Past studies using AFM and quartz crystal microbalance (QCM) have shown that increased vesicle deformation (or flattening) was observed as ligand density was increased, leading ultimately to bilayer formation.[24] To investigate the effect of varying biotin-DOPE mole fraction in the vesicles (0.1 mM total phospholipid concentration), we prepared vesicles with mole fractions of biotin that ranged from 0.1% to 5% and measured the amount of phospholipid captured on the avidin-functionalized surfaces (Figure 6a-c).

Inspection of Figure 6a-c reveals that the amount of phospholipid captured on the surfaces increased with increasing mole fraction of biotinylated lipid. A surprising observation,

however, was the low level of capture of vesicles containing 0.1% biotin-DOPE. To provide insight into this trend, we calculated the availability of biotin groups on the surfaces of these vesicles. Using an average vesicle diameter of 130 nm, and by assuming that the packing density of phospholipid within the vesicle bilayer is that of DOPC in the liquid crystalline phase L_α (0.70 nm^2 per phospholipid[39]), the number of phospholipid molecules in the outer leaf of each vesicle was calculated to be 76,000. From this result, we calculated that 76 biotin groups, on average, are exposed at the surfaces of vesicles that contain 0.1 mol % biotin-DOPE. We conclude therefore that vesicles containing 0.1% biotinylated lipid should present multiple biotin groups for binding to the avidin-functionalized surfaces. We also determined that diffusion of phospholipids[49] across the vesicles occurs on times that are short compared to the duration of our experiments ($D \sim 10^{-12}$ m^2/sec, $t \sim 10^{-3}$ sec), and hence should not be a limiting factor. Thus, the low level of capture of vesicles containing 0.1 mol % biotin-DOPE that is shown in Figure 6 is an unexpected observation. We do not yet understand the reason for this result, although we note that capture of vesicles with low biotin mole fractions (0.3%) has been reported in other studies.[26] We comment, however, that both the procedure used to immobilize the avidin as well as the composition of the lipid in the vesicles used in the prior studies differ from our investigation.[26]

Finally, we note that by increasing the mole fraction of biotinylated lipid within the vesicles above 10% (Figure S7), a saturated coverage of 4.0 ± 0.3 phospholipid molecules/nm^2 was obtained on the avidin-functionalized surfaces. This value coincides with the density of phospholipid on a surface with bilayer coverage. Pignataro *et al.* investigated adhesion of vesicles comprising 5 to 30 mol% of biotinylated lipids to streptavidin-functionalized surfaces.[24] They found that, with increasing biotin concentration, establishment of an increasing number of biotin-streptavidin bonds leads to an increase in overall contact area up to the point where vesicle rupture occurs and the vesicles spread to form planar bilayers. Our results are consistent with this physical picture. We also comment that the saturation coverage of 4.0 ± 0.3 phospholipid molecules/nm^2 achieved by using 20% biotin-DOPE in the vesicles is less than the saturation coverage of 5.1 ± 0.2 phospholipid molecules/nm^2 obtained using 1% biotin-DOPE and vesicle solutions containing high concentrations of phospholipids (>0.5 mM; Figure S6). These two results are consistent with our conclusion that the latter limit is set by the random close-packing of intact vesicles at the surface whereas the former is set by the density of lipid within a bilayer that forms spontaneously at the interface during incubation with the biotinylated vesicles.

We also examined the ordering of 5CB on avidin-functionalized surfaces that were incubated against vesicles containing different mole fractions of biotinylated lipid. Consistent with the above findings, the ordering of the 5CB correlated closely to the density of phospholipid captured on the surfaces (Figure 6d-g; see also Supporting Information for discussion). Indeed, we have found that the data in Figures 5 and 6 can be collapsed onto a single “universal” curve (Figure 7), confirming that the influence of various key parameters (total phospholipid in solution; % biotinylated lipid in the vesicles) on the LC ordering transitions, as reported in this paper, can be largely understood via the effects of those parameters on the amount of phospholipid captured on the surface.

Discussion

This report describes ordering transitions in nematic phases of 5CB induced by surfaces onto which phospholipid vesicles are captured via specific biomolecular interactions. As detailed in the Introduction, the study was motivated by various past observations that the tails of amphiphiles presented at interfaces can dictate the orientational ordering of LCs.[11,15-18] Subsequently, Kuhnau *et al.* used differential scanning calorimetry (DSC) to determine that LCs penetrate into dipalmitoylphosphatidylcholine (DPPC) bilayers, leading to a change in

the ordering of the acyl chains of DPPC.[50,51] Finally, in a recent and elegant experiment, Fletcher *et al.* reported that UV polymerization of the tails of surfactants at aqueous-LC interfaces frustrates homeotropic ordering of the LC whereas polymerization of the headgroup does not perturb the system from the homeotropic orientation.[19] All these experiments support the view that homeotropic anchoring of LCs on lipid-decorated surfaces is induced by the interdigitation (or penetration) of mesogens into the aliphatic chains of the amphiphiles.

In contrast to the above studies, in our work, phospholipids were captured onto surfaces as bilayers of vesicles. Thus, it was not obvious to us at the outset of this study that LCs would order on these surfaces in ways that are similar to surfaces presenting monolayers of lipid acyl side chains. However, our observations of a homeotropic orientation suggest that the ordering of the LC in our study is the result of the interaction of 5CB with the acyl tails of the phospholipids. Reorganization of the bilayer to enable this interaction likely happens before (i.e., upon exposure to air) and/or upon contact with the LC. The conclusion that lipid acyl chain-LC interaction dominates the LC ordering in our studies is further supported our observation that the surface density of phospholipid required to trigger the ordering transition of 5CB in our system (1.8 molecules/nm^2; see Figure 7) was close to monolayer coverage. Previous studies using supported monolayers in which the aliphatic side chains of the phospholipid molecules at the interface dictate the homeotropic ordering of 5CB have also found that near monolayer coverages of lipid are needed to cause the homeotropic orientation. We note that the reorganization of the phospholipids that we infer to take place on the surfaces used in our study will, in general, be influenced by a variety of factors including adhesion energy, external pressure and bending rigidity of the membrane of the vesicles as well as the phase state of the lipid in the bilayers.[52] Thus, future studies using other lipids (e.g., DPPC with a melting temperature of 41°C) will be required to establish the generality of the observations reported in the current manuscript using DOPC-rich vesicles.

As described above, in the absence of captured vesicles, the alignment of 5CB on the avidin-functionalized surface was planar. In contrast, specific binding of phospholipid vesicles to the avidin functionalized surface led to a distinct state of ordering of the LC that is attributed to coupling of phospholipid on surfaces with 5CB. Because all protein-presenting surfaces characterized to date give rise to planar alignment of LCs[8,9,12], this suggests that proteins (including antibodies) can be utilized as binding groups to facilitate specific capture of a range of phospholipid complexes, and that the orientational ordering of LCs on protein-coated surfaces provides a broadly useful approach for reporting molecular recognition events between proteins and phospholipid-containing complexes. In future studies, we aim to extend our investigations to the capture of native vesicles shed by mammalian cells.

Although the generality of our observations remains to be established, we note that ordering transitions in LCs have been reported on surfaces decorated with complex biological structures comprised of lipids. For example, several viruses that possess phospholipid envelopes, when adsorbed to surfaces, were demonstrated to cause homeotropic alignment of 5CB. Because near-planar alignment of LCs was observed when non-enveloped viruses were presented at surfaces, the authors attributed the observed homeotropic alignment of 5CB to the interactions of 5CB and the lipid envelopes of the viruses.[13] In contrast to our study, however, the viruses used in the prior studies were not captured on the surfaces by specific binding events. Because the bilayers of enveloped viruses as well as native microvesicles are derived from the membranes of mammalian cells (and thus comprise a complex mixture of lipids, proteins and polysaccharides), the results described above do hint that native vesicles may trigger ordering transitions in LCs.

A key observation made in this paper is that the ordering transition of the LC is a discontinuous function of the surface density of phospholipid captured on the surface.[53] In general, the interaction between a surface and nematic phase is characterized by an orientation-dependent surface free energy defined by the expression $F(\theta) = (W / 2) \sin^2(\phi - \theta)$, where W is the so-called anchoring strength, ϕ is the preferred anchoring angle at the surface (referred to as "easy axis") and θ is the actual angle of the director at the surface.[54] Minimization of both the orientation-dependent free energy of the LC at the surface and the elastic energy of the LC within the bulk gives rise to the equilibrium director profile. Whether or not a continuous or discontinuous transition in orientational ordering of a LC is observed can be determined by manipulating the relative anchoring strength of a surface and the nematic elasticity. We speculate that because the LC ordering transition reported in this paper is discontinuous, the elastic energy associated with the strain of the LC is small compared to surface anchoring. In a future study, we will design an experimental system that will seek to balance elastic and surface effects to achieve a continuous transition in ordering of the LC. We note that several groups have reported a continuous range of pretilt angles of LCs on surfaces.[55-57] For example, Clare *et al.* observed continuous changes in the orientations of LCs across surfaces with continuous gradients in surface chemistry.[58]

Conclusion

We derive three primary conclusions from the study reported in this paper. First, we conclude that ordering transitions in nematic phases of 5CB can be induced by the capture of phospholipid vesicles at surfaces via specific recognition events. Because surfaces decorated with proteins give rise to parallel orientations of nematic 5CB, the capture of phospholipid at the avidin-decorated surface results in an ordering transition in the 5CB to the homeotropic orientation and a distinct change in the optical appearance of the LC. These ordering transitions hint at the basis of a physicochemical phenomenon that may permit facile reporting of the presence of a range of lipid complexes captured through specific binding events on protein-functionalized surfaces.

Second, our results are consistent with a physical picture in which the aliphatic side chains of the phospholipids captured at the surfaces (as either vesicles or planar multilayer assemblies) dictate the ordering of the LC. In order for this interaction to take place, we conclude that the phospholipid assemblies captured initially at the surfaces must reorganize. Indeed, we observed reorganization of the phospholipid assemblies by AFM (e.g., vesicles to planar bilayer assemblies), although additional experiments are required to characterize the exact organization of the lipid acyl chains in contact with the LC. A significant result of our study is the observation that the vesicle-to-planar bilayer transition seen by AFM does not lead to a substantial loss of phospholipid from the surface (<10%). We also determined that a minimum surface density of 1.8 phospholipid molecules/nm^2 was required to trigger homeotropic ordering of the nematic LC in our study. Because this surface density of lipid is close to that required to cause homeotropic ordering of 5CB in studies based on monolayers that are designed to present the lipid acyl groups to the LC,[11,15,16,18] this result further supports our hypothesis that interactions of 5CB and the acyl chains of captured phospholipids lead to the ordering transition observed in this study.

A third significant conclusion of the study reported herein is related to the maximum density of lipid captured by the specific binding of vesicles at surfaces. For vesicles containing 1% biotin-DOPE, AFM revealed the capture of intact vesicles at the surface in buffer and a maximum lipid loading set by random close-packed vesicles on the surface (5.1 ± 0.2 phospholipid molecules/nm^2) was measured by quantitative fluorimetry. At high concentrations of biotinylated lipid (>10%) in the vesicles, however, the limiting lipid loading was 4.0 ± 0.3 phospholipid molecules/nm^2, consistent with spontaneous formation

of a bilayer during incubation with the biotinylated vesicles. In both cases, homeotropic ordering of the LC was observed, consistent with the above-mentioned reorganization of lipid on the surface leading to interaction of the acyl side chains of the lipid with the LC.

Supplementary Material

Refer to Web version on PubMed Central for supplementary material.

Acknowledgments

The authors acknowledge Aaron Lowe and Jacob Hunter for helpful comments on this manuscript. This research was partially supported by the National Science Foundation (DMR 0079983) and the National Institutes of Health (CA108467 and CA105730).

References

1. Thery C, Ostrowski M, Segura E. Nature Reviews Immunology 2009;9:581–593.
2. Ratajczak J, Wysoczynski M, Hayek F, Janowska-Wieczorek A, Ratajczak MZ. Leukemia 2006;20:1487–1495. [PubMed: 16791265]
3. Al-Nedawi K, Meehan B, Micallef J, Lhotak V, May L, Guha A, Rak J. Nature Cell Biology 2008;10:619–624.
4. Al-Nedawi K, Meehan B, Rak J. Cell Cycle 2009;8:2014–2018. [PubMed: 19535896]
5. Luk YY, Yang KL, Cadwell K, Abbott NL. Surface Science 2004;570:43–56.
6. Shah RR, Abbott NL. J Phys Chem B 2001;105:4936–4950.
7. Shah RR, Abbott NL. Science 2001;293:1296–1299. [PubMed: 11509724]
8. Skaife JJ, Abbott NL. Langmuir 2001;17:5595–5604.
9. Gupta VK, Skaife JJ, Dubrovsky TB, Abbott NL. Science 1998;279:2077–2080. [PubMed: 9516101]
10. Price AD, Schwartz DK. Journal of the American Chemical Society 2008;130:8188–8194. [PubMed: 18528984]
11. Brake JM, Daschner MK, Luk YY, Abbott NL. Science 2003;302:2094–2097. [PubMed: 14684814]
12. Jang CH, Tingey ML, Korpi NL, Wiepz GJ, Schiller JH, Bertics PJ, Abbott NL. Journal of the American Chemical Society 2005;127:8912–8913. [PubMed: 15969543]
13. Jang CH, Cheng LL, Olsen CW, Abbott NL. Nano Letters 2006;6:1053–1058. [PubMed: 16683850]
14. Chen CH, Yang KL. Langmuir 2010;26:1427–1430. [PubMed: 19961190]
15. Hiltrop K, Stegemeyer H. Berichte Der Bunsen-Gesellschaft-Physical Chemistry Chemical Physics 1978;82:884–889.
16. Hiltrop K, Stegemeyer H. Berichte Der Bunsen-Gesellschaft-Physical Chemistry Chemical Physics 1981;85:582–588.
17. Lockwood NA, Abbott NL. Current Opinion in Colloid & Interface Science 2005;10:111–120.
18. Meli MV, Lin IH, Abbott NL. J Am Chem Soc 2008;130:4326–4333. [PubMed: 18335929]
19. Fletcher PDI, Kang NG, Paunov VN. ChemPhysChem 2009;10:3046–3053. [PubMed: 19780096]
20. Reimhult E, Hook F, Kasemo B. Langmuir 2003;19:1681–1691.
21. Schonherr H, Johnson JM, Lenz P, Frank CW, Boxer SG. Langmuir 2004;20:11600–11606. [PubMed: 15595789]
22. Richter RP, Berat R, Brisson AR. Langmuir 2006;22:3497–3505. [PubMed: 16584220]
23. Patolsky F, Lichtenstein A, Willner I. J Am Chem Soc 2000;122:418–419.
24. Pignataro B, Steinem C, Galla HJ, Fuchs H, Janshoff A. Biophysical Journal 2000;78:487–498. [PubMed: 10620312]
25. Boukobza E, Sonnenfeld A, Haran G. J Phys Chem B 2001;105:12165–12170.

26. Jung LS, Shumaker-Parry JS, Campbell CT, Yee SS, Gelb MH. J Am Chem Soc 2000;122:4177–4184.
27. Berquand A, Mazeran PE, Pantigny J, Proux-Delrouyre V, Laval JM, Bourdillon C. Langmuir 2003;19:1700–1707.
28. Lowe AM, Ozer BH, Wiepz GJ, Bertics PJ, Abbott NL. Lab on a Chip 2008;8:1357–1364. [PubMed: 18651079]
29. Provencher SW. Computer Physics Communications 1982;27:213–227.
30. Provencher SW. Comput Phys Commun 1982;27:229–242.
31. Clare BH, Abbott NL. Langmuir 2005;21:6451–6461. [PubMed: 15982053]
32. Lin IH, Meli MV, Abbott NL. Journal of Colloid And Interface Science 2009;336:90–99. [PubMed: 19428021]
33. Bloss, FD. An Introduction to the Methods of Optical Crystallography. Holt, Rinehart and Winston; New York: 1961.
34. He XM, Carter DC. Nature 1992;358:209–215. [PubMed: 1630489]
35. Green NM, Joynson MA. Biochemical Journal 1970;118:71. [PubMed: 5472157]
36. Silvius, JR. Thermotropic Phase Transitions of Pure Lipids in Model Membranes and Their Modifications by Membrane Proteins. John Wiley and Sons; New York: 1982.
37. Dufrene YF, Barger WR, Green JBD, Lee GU. Langmuir 1997;13:4779–4784.
38. Markiewicz P, Goh MC. Langmuir 1994;10:5–7.
39. Nagle JF, Tristram-Nagle S. Biochim Biophys Acta 2000;1469:159–195. [PubMed: 11063882]
40. Cohen FS, Akabas MH, Finkelstein A. Science 1982;217:458–460. [PubMed: 6283637]
41. Seitz M, Ter-Ovanesyan E, Hausch M, Park CK, Zasadzinski JA, Zentel R, Israelachvili JN. Langmuir 2000;16:6067–6070. [PubMed: 20953315]
42. Olbrich K, Rawicz W, Needham D, Evans E. Biophysical Journal 2000;79:321–327. [PubMed: 10866958]
43. Ross EE, Bondurant B, Spratt T, Conboy JC, O'Brien DF, Saavedra SS. Langmuir 2001;17:2305–2307.
44. Solletti JM, Botreau M, Sommer F, Brunat WL, Kasas S, Duc TM, Celio MR. Langmuir 1996;12:5379–5386.
45. Brake JM, Mezera AD, Abbott NL. Langmuir 2003;19:8629–8637.
46. Ferri JK, Stebe KJ. Advances in Colloid and Interface Science 2000;85:61–97. [PubMed: 10696449]
47. Lucero A, Nin o MRR, Gunning AP, Morris VJ, Wilde PJ, Patino JMR. J Phys Chem B 2008;112:7651–7661. [PubMed: 18517243]
48. Zhdanov VP, Keller CA, Glasmästar K, Kasemo B. The Journal of Chemical Physics 2000;112:900–909.
49. Filippov A, Orädd G, Lindblom G. Biophysical Journal 2003;84:3079–3086. [PubMed: 12719238]
50. Kühnau U, Mädler B, Wurlitzer S, Rapp G, Schmiedel H. Mol Cryst Liq Cryst 1997;304:171–178.
51. Kühnau U, Petrov AG, Klose G, Schmiedel H. Physical Review E 1999;59:578–585.
52. Seifert U, Lipowsky R. Physical Review A 1990;42:4768–4771. [PubMed: 9904586]
53. Xue CY, Yang KL. Langmuir 2008;24:563–567. [PubMed: 18095723]
54. Barbero G, Barberi R. J Phys (Paris) 1983;44:609–616.
55. Sinha GP, Wen B, Rosenblatt C. Applied Physics Letters 2001;79:2543–2545.
56. Vaughn KE, Sousa M, Kang D, Rosenblatt C. Applied Physics Letters 2007;90:194102.
57. Price AD, Schwartz DK. Langmuir 2006;22:9753–9759. [PubMed: 17073507]
58. Clare BH, Efimenko K, Fischer DA, Genzer J, Abbott NL. Chemistry of Materials 2006;18:2357–2363.

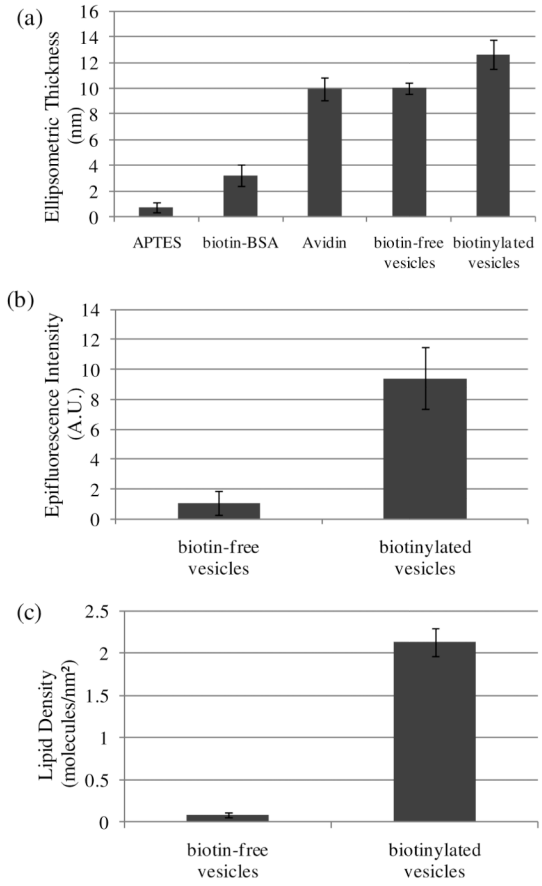

Figure 1.

(a) Ellipsometric thicknesses of APTES, biotin-BSA, avidin and a dispersion of vesicles deposited sequentially onto a silicon wafer. The biotin-free vesicles were composed of 99% DOPC, 1% BODIPY-DHPE; the biotinylated vesicles were composed of 98% DOPC, 1% biotin-DOPE, 1% BODIPY-DHPE. (b) Plot of epifluorescence intensity measured following incubation of an avidin-functionalized glass slide in a dispersion of vesicles. (c). Plot of lipid density measured following incubation of an avidin-functionalized glass slide in a dispersion of vesicles. The error bars represent one standard deviation. (N=4)

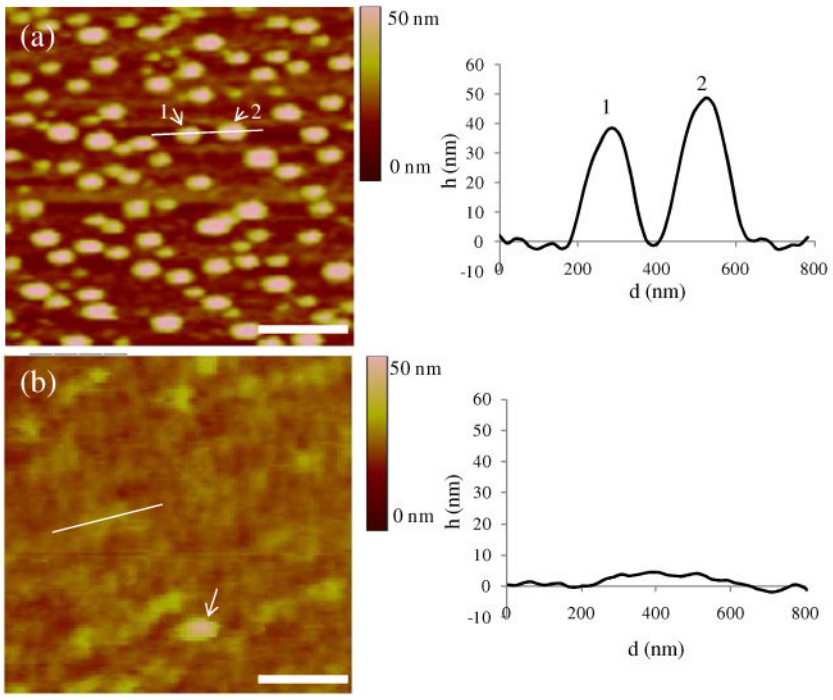

Figure 2.

AFM images of biotinylated vesicles captured on an avidin-functionalized surface after (a) rinsing in TBS and (b) rinsing in water. In (b), the line corresponds to the location of the measurement of the cross sectional height (right plot), and the arrow indicates the existence of an intact vesicle. (scale bar = 500 nm)

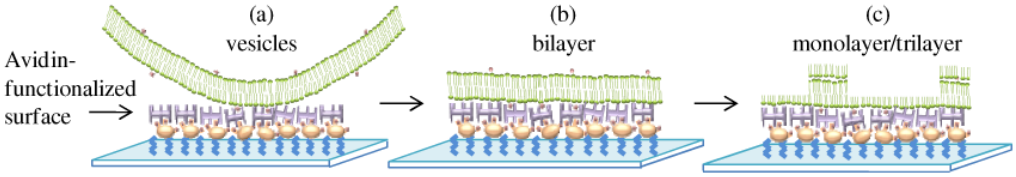

Figure 3.
Schematic illustration of the morphological states of phospholipids captured on the avidin-functionalized surfaces after (a) rinsing in TBS, (b) rinsing in water and (c) drying.

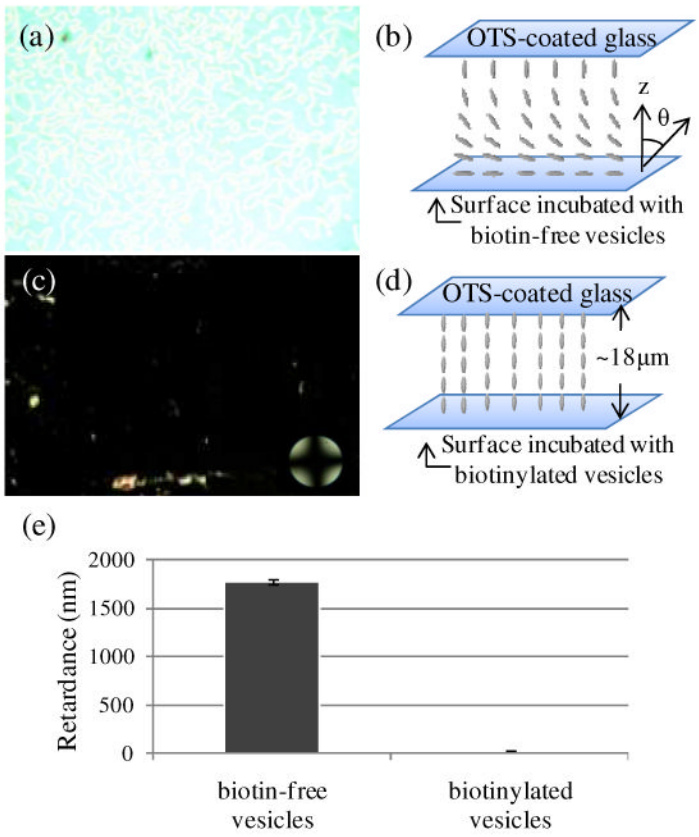

Figure 4.

(a) Optical image (crossed polars) of nematic 5CB sandwiched in an optical cell with an avidin-functionalized surface that was incubated against biotin-free vesicles. (b) Schematic illustration of the planar alignment of the LC in contact with the avidin-functionalized surface. The OTS-treated glass causes homeotropic anchoring of 5CB. (c) Optical image (crossed polars) of nematic 5CB sandwiched in an optical cell with an avidin-functionalized surface that was incubated against biotinylated vesicles. (d) Schematic illustration of the homeotropic anchoring of the LC on the surface incubated with biotinylated vesicles. (e) Optical retardance of the 5CB films described in (a) and (c). The error bars represent one standard deviation. (N=4)

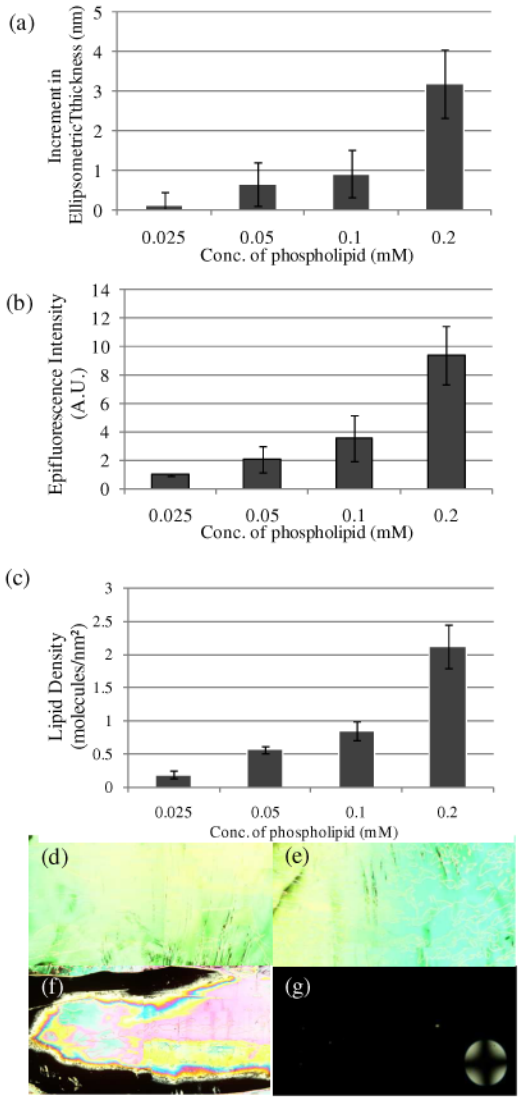

Figure 5.

(a) Increment in optical thickness following incubation of biotinylated vesicles on avidin-functionalized surfaces, as a function of total phospholipid concentration in solution (1 mol % biotin-DOPE). (b) Plot of epifluorescence intensity of surfaces measured following incubation in various concentrations of biotinylated vesicles. (c) Plot of lipid density on the surfaces measured following incubation in various concentrations of biotinylated vesicles. Optical images (crossed polars) of nematic 5CB sandwiched in optical cells with surfaces incubated with biotinylated vesicle solutions with total lipid concentrations of (d) 0.025 mM, (e) 0.05 mM, (f) 0.1 mM and (g) 0.2 mM. The error bars represent one standard deviation. (N=4)

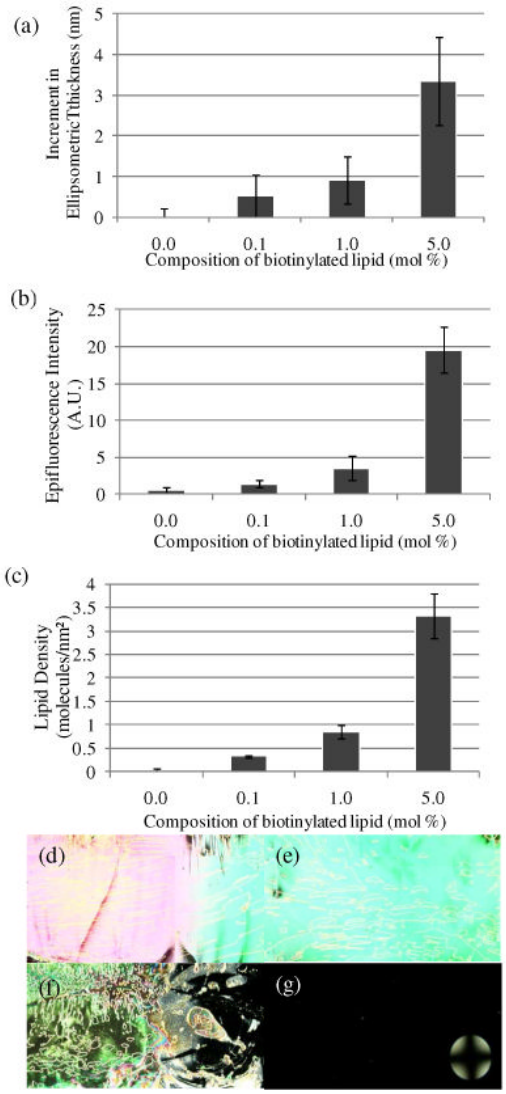

Figure 6.

(a) Increment in optical thickness following incubation of vesicles on avidin-functionalized surfaces, as a function of mole fraction of biotinylated lipid (0.1 mM total lipid concentration in solution). (b) Plot of epifluorescence intensity of surfaces measured following incubation of vesicles, as a function of mole fraction of biotinylated lipid. (c) Plot of lipid density measured following incubation of vesicles, as a function of mole fraction of biotinylated lipid. Optical images (crossed polars) of nematic 5CB sandwiched in optical cells with surfaces incubated with solutions of vesicles with (d) 0 mol %, (e) 0.1 mol %, (f) 1 mol % and (g) 5 mol % of biotinylated lipid. The error bars represent one standard deviation. (N=4)

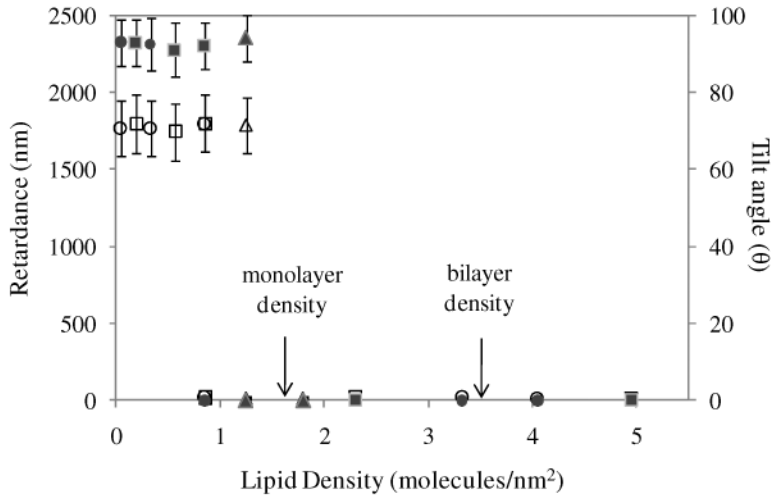

Figure 7.

Plot of optical retardance of nematic films of 5CB (solid symbols) and tilt angle of 5CB (hollow symbols) at the avidin-functionalized surface on which vesicles were incubated versus density of phospholipid captured on the surface. Squares represent data obtained from surfaces incubated with varying total phospholipid concentration (1 mol % biotinylated lipid); Circles represent data obtained by varying mole fraction of biotinylated lipid (total concentration of phospholipid of 0.1 mM); Triangles represent data obtained by varying the time of incubation of the vesicles in solution (see Figure S8). The error bars represent one standard deviation.